

# Superfluid-Mott Insulator Transition of Spin-2 Cold Bosons in an Optical Lattice in a Magnetic Field

Shuo Jin<sup>1\*</sup>, Jing-Min Hou<sup>1</sup> †, Bing-Hao Xie<sup>2</sup>, Li-Jun Tian<sup>1</sup>, and Mo-Lin Ge<sup>1</sup>

<sup>1</sup>*Theoretical Physics Division, Nankai Institute of Mathematics,*

*Nankai University, Tianjin, 300071, China, and*

*Liuhui Center for Applied Mathematics, Tianjin, 300071, China*

<sup>2</sup>*Laboratory for Computational Physics,*

*Institute of Applied Physics and Computational Mathematics, Beijing, 100088, China*

## Abstract

The superfluid-Mott insulator transition of spin-2 boson atoms with repulsive interaction in an optical lattice in a magnetic field is presented. By using the mean field theory, Mott ground states and phase diagrams of superfluid-Mott insulator transition at zero temperature are revealed. Applied magnetic field leads to some phase boundaries splitting. For all the initial Mott ground states containing multiple spin components, different spin components take on different phase boundaries. It is found that in this system the phase boundaries with different magnetization can be moved in different ways by only changing the intensity of the applied magnetic field.

PACS number(s): 03.75.Kk, 03.75.Lm, 03.75.Mn, 32.80.Pj

---

\* Electronic address: jinshuo@eyou.com

† Electronic address: jmhous@eyou.com

## I. INTRODUCTION

Recent remarkable experiments [1, 2, 3, 4] on the superfluid (SF) to Mott insulator (MI) transition in a system of ultracold atoms in an optical lattice open intriguing prospects for studying many-body phenomena, associated with strongly correlated systems in a highly controllable environment. The optical lattices [5, 6]—arrays of microscopic potentials induced by the ac stark effect of interfering laser beams—provide ideal conditions for the study of the laser cooling and the quantum phase transitions of the confined cold atoms. The dynamics of the confined atoms in optical lattices is adequately described by the Bose-Hubbard model [7, 8], which predicts SF-MI transition at low temperature with increasing the ratio of the on-site interaction to the hopping matrix element. Besides many experimental efforts made to realize SF-MI transition, a large number of theoretical studies have appeared [7, 8, 9, 10]. In reference [9] an appropriate mean-field approximation was developed for the Hamiltonian of spinless or polarized bosons in an optical lattice, and in order to describe the zero-temperature phase transition from the superfluid to the Mott-insulating phase, the phase diagrams were calculated.

Since optical traps [11, 12, 13] liberate the spin degrees of freedom and make possible condensation of spinor bosons, extensive interests have been stimulated in the study of multi-component spinor BEC. The quantum phase transition in spinor BEC, as well as a variety of other novel phenomena [14, 15, 16, 17, 18] were well studied. Subsequently, inspired by these works, the theoretical researches about the SF-MI transition of the spinor bosons trapped in an optical lattice arise. Most recently, Demler and Zhou [19] have studied spin-1 Bose atoms in an optical lattice and obtained several unique properties. Tsuchiya *et al.* [20], Hou and Ge [21] have investigated the spin-1 and spin-2 bosons in an optical lattice with the mean-field approximation method and obtained the phase diagrams showing a transition from Mott insulator to superfluid, respectively.

On the other hand, the response to external magnetic field of BEC is also a topic with interests [17, 18, 22, 23, 24, 25]. The experimentalists have concentrated on investigating the systems in an applied magnetic field because the phase transition can be tuned by adjusting the magnetic field rather than changing the samples measured [26, 27, 28, 29]. Thus the theoretical study in this aspect is necessary. So far, Ueda and Koashi [17, 18] have discussed the magnetic response of spin-1 and spin-2 BEC in a mesoscopic regime; as to the system in an optical lattice, Svicinsky and Chui [30] have studied the spin-1 bosons in a magnetic field and shown

some effects induced by the magnetic field. However, the spin-2 case in a magnetic field has not been discussed yet. What about the ground states, quantum phase transition and the influence of the magnetic field on this system? This is our mission in the present letter. First, ignoring the hopping term of the Hamiltonian, we get the site-independent Hamiltonian, its energy eigenvalues and the Mott ground states for different cases. Then, applying mean-field approximation and regarding the hopping term as a perturbation, we perform the calculations in second-order and draw the phase diagrams. The response of the phase diagrams to the applied magnetic field is qualitatively analyzed subsequently. Finally, we give some remarks and the conclusion.

## II. THE MODEL

We consider a dilute gas of boson atoms with hyperfine spin  $F = 2$ , such as  $^{23}\text{Na}$ ,  $^{87}\text{Rb}$  or  $^{85}\text{Rb}$  subject to an external magnetic field in an optical lattice. Based on Ref. [21], the Hamiltonian of spin-2 bosons with repulsive interaction in an optical lattice including a magnetic field term can be written in the second-quantized form:

$$H = H_A + H_B, \quad (1)$$

$$H_A = \int d\mathbf{r} \left[ \frac{\hbar}{2M} \nabla \Psi_\alpha^\dagger \cdot \nabla \Psi_\alpha + V(\mathbf{r}) \Psi_\alpha^\dagger \Psi_\alpha - \bar{\mu} \Psi_\alpha^\dagger \Psi_\alpha + \frac{\bar{c}_0}{2} \Psi_\alpha^\dagger \Psi_\beta^\dagger \Psi_\beta \Psi_\alpha \right. \\ \left. + \frac{\bar{c}_1}{2} \sum_i (\Psi_\alpha^\dagger (F_i)_{\alpha\beta} \Psi_\beta)^2 + \bar{c}_2 \Psi_\alpha^\dagger \Psi_{\alpha'}^\dagger \langle 2\alpha; 2\alpha' | 00 \rangle \langle 00 | 2\beta; 2\beta' \rangle \Psi_\beta \Psi_{\beta'} \right], \quad (2)$$

$$H_B = -\mu_B g \int d\mathbf{r} \Psi_\alpha^\dagger (\mathbf{B} \cdot \mathbf{F})_{\alpha\beta} \Psi_\beta, \quad (3)$$

where  $V(\mathbf{r}) = V_0(\sin^2 kx + \sin^2 ky + \sin^2 kz)$  with  $k$  the wave vector of the laser light and  $V_0$  a tunable amplitude characterizing an optical lattice,  $B$  is a uniform magnetic field independent of time,  $\mu_B$  is the Bohr magneton and  $g$  is the Lande factor of an atom,  $M$  is the atomic mass,  $\Psi_{+2}, \dots, \Psi_{-2}$  are the five-component field operators corresponding to the sublevels  $m_F = +2, \dots, -2$  of the hyperfine state  $F = 2$ ,  $\bar{\mu}$  is the chemical potential,  $\bar{c}_0 = 4\pi\hbar^2(3a_4 + 4a_2)/7m$ ,  $\bar{c}_1 = 4\pi\hbar^2(a_4 - a_2)/7m$  and  $\bar{c}_2 = 4\pi\hbar^2(3a_4 - 10a_2 + 7a_0)/7m$  are parameters related to s-wave scattering lengths  $a_0$ ,  $a_2$  and  $a_4$  of the two colliding bosons with total angular momenta 0, 2 and 4,  $\langle 2\alpha; 2\alpha' | 00 \rangle$  and  $\langle 00 | 2\beta; 2\beta' \rangle$  are Clebsch-Gordan coefficients.  $F_\alpha (\alpha = x, y, z)$  are  $5 \times 5$  spin matrices obeying usual momentum commutation relations  $[F_\alpha, F_\beta] = \epsilon_{\alpha\beta\gamma} F_\gamma$ .

For simplicity, we assume a uniform magnetic field applied along the  $z$ -direction, and it is weak enough to ignore the quadratic Zeeman effect. Expanding the field operators in the Wannier basis and keeping only the lowest vibrational states,  $\Psi_\alpha = \sum_i b_{i\alpha} w(\mathbf{r} - \mathbf{r}_i)$ , Eq. (1) reduces to the generalized Bose-Hubbard Hamiltonian

$$H = -t \sum_{\langle i,j \rangle} b_i^\dagger b_j - \mu \sum_i \hat{n}_i + \frac{c_0}{2} \sum_i \hat{n}_i (\hat{n}_i - 1) + \frac{c_1}{2} \sum_i (\hat{\mathbf{F}}_i^2 - 6\hat{n}_i) + \frac{2c_2}{5} \sum_i \hat{S}_{i+} \hat{S}_{i-} - \sum_i p \hat{F}_{zi}, \quad (4)$$

where  $\hat{\mathbf{F}}_i = b_{i\alpha}^\dagger \mathbf{F}_{\alpha\beta} b_{i\beta}$ ,  $\hat{n}_i = \sum_\alpha b_{i\alpha}^\dagger b_{i\alpha}$ ,  $t = -\int d\mathbf{r} w_i^*(\mathbf{r}) (-\hbar^2 \nabla^2 / 2m + V(\mathbf{r})) w_i(\mathbf{r})$  is the hopping matrix element between adjacent sites  $i$  and  $j$ ,  $\mu = \bar{\mu} \int d\mathbf{r} |w_i(\mathbf{r})|^2 + \int d\mathbf{r} w_i^*(\mathbf{r}) (-\hbar^2 \nabla^2 / 2m + V(\mathbf{r})) w_i(\mathbf{r})$  describes the effective chemical potential, and  $c_i = \bar{c}_i \int d\mathbf{r} |w_i(\mathbf{r})|^4$  is on-site inter-atom interaction, where the Hubbard approximation has been used to treat the multi-center integral as a single-center one.  $\hat{S}_{i+} = \hat{S}_{i-} = (b_{i0}^\dagger)^2 / 2 - b_{i1}^\dagger b_{i-1}^\dagger + b_{i2}^\dagger b_{i-2}^\dagger$  creates a spin-singlet “pair” when applied to the vacuum, and we further assume  $p = g\mu_B B > 0$  in the following discussion.

In the limit  $c_0/t \rightarrow \infty$ , the hopping term can be neglected, so the Hamiltonian is reduced to a diagonal matrix with respect to sites. Then the single-site Hamiltonian is

$$h_0 = -\mu \hat{n} + \frac{c_0}{2} \hat{n} (\hat{n} - 1) + \frac{c_1}{2} (\hat{\mathbf{F}}^2 - 6\hat{n}) + \frac{2c_2}{5} \hat{S}_+ \hat{S}_- - p \hat{F}_z. \quad (5)$$

For the sake of studying the quantum transition, the mean-field approximation [9] is used and the hopping term is considered as a perturbation. Introducing the superfluid order parameter  $\phi_\alpha = \langle b_{i\alpha} \rangle = \sqrt{n_{sf}} \zeta_\alpha$  ( $n_{sf}$  is the superfluid density and  $\zeta_\alpha$  is a normalized spinor  $\zeta_\alpha^* \zeta_\alpha = 1$ ), we decouple the hopping term as  $b_{i\alpha}^\dagger b_{j\alpha} \approx (\phi_\alpha b_{i\alpha}^\dagger + \phi_\alpha^* b_{j\alpha}) - \phi_\alpha^* \phi_\alpha$ , then, the total hopping term becomes the product of a site-independent term and the total number of the sites. As a result, we only consider a single site because the Hamiltonian of every site is identical in the homogenous case, and the Hamiltonian is represented by a site-independent effective Hamiltonian multiplied by the total number of sites. The Hamiltonian of a single site reads

$$h = h_0 + h_1, \quad (6)$$

$$h_1 = zt(\phi_\alpha b_\alpha^\dagger + \phi_\alpha^* b_\alpha - \phi_\alpha^* \phi_\alpha), \quad (7)$$

where  $h_1$  is the mean-field version of the hopping Hamiltonian in the single site, and  $z$  is the number of the nearest-neighbor sites. When the ratio  $c_0/t$  is very large,  $h_1$  is considered as a perturbation term.

### III. THE ENERGY EIGENVALUES AND THE MOTT GROUND STATES

Before perturbative calculations, we solve the equation

$$h_0\psi = \varepsilon^{(0)}\psi \quad (8)$$

to get the eigenvalues and eigenstates of  $h_0$ . In Eq. (5), the operators  $\hat{S}_+$  and  $\hat{S}_-$  satisfy the  $SU(1, 1)$  commutation relations, namely  $[\hat{S}_z, \hat{S}_\pm] = \pm \hat{S}_\pm$ ,  $[\hat{S}_+, \hat{S}_-] = -2\hat{S}_z$  together with  $\hat{S}_z \equiv (2\hat{n} + 5)/4$ , and as a consequence, the Casimir operator  $\hat{\mathbf{S}}^2 \equiv -\hat{S}_+\hat{S}_- + \hat{S}_z^2 - \hat{S}_z$  commutes with  $\hat{S}_\pm$  and  $\hat{S}_z$  [17, 18]. The eigenvalues of the mutual eigenstates for  $\hat{\mathbf{S}}^2$  and  $\hat{S}_z$  are  $\{S(S-1), S_z\}$  with  $S = (2n_0 + 5)/4$  ( $n_0 = 0, 1, 2, \dots$ ) and  $S_z = S + n_s$  ( $n_s = 0, 1, 2, \dots$ ), which guarantees that  $\hat{S}_+\hat{S}_- = \hat{S}_z^2 - \hat{S}_z - \hat{\mathbf{S}}^2$  is positive semidefinite. The new quantum numbers  $n_s$  and  $n_0$  are introduced and the operator  $S_+$  raises  $n_s$  by one while the relation  $n = 2n_s + n_0$  holds, where  $n$  is the total number of bosons in a single site. The spin operator  $\hat{\mathbf{F}}$  and the magnetic quantum number operator  $\hat{F}_z$  commute with the operators  $\hat{S}_\pm$ , and then, the eigenstates  $\psi$  are denoted as  $|n_0, n_s, F, F_z; \lambda\rangle$  where  $\lambda$  labels orthonormal degenerate states. The energy eigenvalue is given by

$$\varepsilon^{(0)} = -\mu n + \frac{c_0}{2}n(n-1) + \frac{c_1}{2}[F(F+1) - 6n] + \frac{2c_2}{5}n_s(n - n_s + \frac{3}{2}) - pF_z, \quad (9)$$

So Mott states can be expressed as  $\prod_i |n_0, n_s, F, F_z; \lambda\rangle_i$ , where  $i$  is lattice site index. For the homogenous case, the zeroth order total energy is  $E^{(0)} = \sum_i \varepsilon^{(0)} = N_l \varepsilon^{(0)}$ , where  $N_l$  is the number of lattice sites.

The energy eigenstates  $|n_0, n_s, F, F_z; \lambda\rangle$  can be represented as [18]

$$(\hat{F}_-)^{\Delta F} (\hat{A}_0^{(2)\dagger})^{n_{20}} \hat{P}_{(n_s=0)} (b_2^\dagger)^{n_{12}} (\hat{A}_2^{(2)\dagger})^{n_{22}} (\hat{A}_0^{(3)\dagger})^{n_{30}} (\hat{A}_3^{(3)\dagger})^{n_{33}} |vac\rangle, \quad (10)$$

where

$$\hat{A}_0^{(2)\dagger} = \frac{1}{\sqrt{10}}[(b_0^\dagger)^2 - 2b_1^\dagger b_{-1}^\dagger + 2b_2^\dagger b_{-2}^\dagger], \quad (11)$$

$$\hat{A}_2^{(2)\dagger} = \frac{1}{\sqrt{14}}[2\sqrt{2}b_2^\dagger b_0^\dagger - \sqrt{3}(b_1^\dagger)^2], \quad (12)$$

$$\hat{A}_0^{(3)\dagger} = \frac{1}{\sqrt{210}}[\sqrt{2}(b_0^\dagger)^3 - 3\sqrt{2}b_1^\dagger b_0^\dagger b_{-1}^\dagger + 3\sqrt{3}(b_1^\dagger)^2 b_{-2}^\dagger + 3\sqrt{3}b_2^\dagger (b_{-1}^\dagger)^2 - 6\sqrt{2}b_2^\dagger b_0^\dagger b_{-2}^\dagger], \quad (13)$$

$$\hat{A}_3^{(3)\dagger} = \frac{1}{20}[(b_1^\dagger)^3 - \sqrt{6}b_2^\dagger b_1^\dagger b_0^\dagger + 2(b_2^\dagger)^2 b_{-1}^\dagger]. \quad (14)$$

$P_{(n_s=0)}$  is the projection onto the subspace with  $n_s = 0$ ;  $n_{12}, n_{20}, n_{22}, n_{30} = 0, 1, 2, \dots, \infty$ ,  $n_{33} = 0, 1$ , and  $\Delta F = 0, 1, \dots, 2F$  that are related to  $\{n_0, n_s, F, F_z\}$  by

$$n_0 = n_{12} + 2n_{22} + 3n_{30} + 3n_{33}, \quad (15)$$

$$n_s = n_{20}, \quad (16)$$

$$F = 2n_{12} + 2n_{22} + 3n_{33}, \quad (17)$$

$$F_z = F - \Delta F. \quad (18)$$

From Eq. (9), we see that the minimum energy states always satisfy  $F_z = F$  when  $p > 0$ . Thus, the problem of finding the ground states reduces to minimizing the function:

$$\begin{aligned} \varepsilon^{(0)}(F, n_s) = & -\mu n + \frac{c_0}{2}n(n-1) + \frac{c_1}{2}[(F - \frac{2p-c_1}{2c_1})^2 - 6n - \frac{(c_1-2p)^2}{4c_1^3}] \\ & + \frac{2c_2}{5}n_s(n - n_s + \frac{3}{2}). \end{aligned} \quad (19)$$

The ground states of  $h_0$  depend on the relation among  $c_1, c_2, p$  and  $\mu$ . When  $n = 1$ , the ground state is  $|1, 0, 2, 2; \lambda\rangle$ ; when  $n \geq 2$ , there are four sorts of ground states classified by different sign combinations of  $c_1$  and  $c_2$ . Here the classification of the Mott ground states differs from that of Ref. [18], which is labelled by ferromagnetic, antiferromagnetic and cyclic phases. In general, for  $p > 0$ , when  $c_1 < 0, c_2 > 0$  (ferromagnetic case), the third and the fourth term in Eq. (19) possess the minimal values simultaneously, but when  $c_1 < 0, c_2 < 0$  (ferromagnetic or antiferromagnetic case),  $c_1 > 0, c_2 > 0$  (ferromagnetic or cyclic case) and  $c_1 > 0, c_2 > 0$  (ferromagnetic or antiferromagnetic case), the situation becomes complicated, since sometimes there exists the competition between contributions of total spin and the singlet “pairs” to eigenenergy. We list all Mott ground states in detail in appendix.

#### IV. PHASE DIAGRAMS OF SUPERFLUID-MOTT INSULATOR TRANSITION

From Section III, we know that  $F = F_z$  always holds in the ground states, while in the excited states this is not the case. As a result of the applied magnetic field, the state degeneracy from the different magnetic quantum numbers  $F_z$  [21] is lifted. More rich phase diagrams are expected than those in the absence of the magnetic field.

To depict the phase diagrams, we consider the hopping term as the perturbative one and calculate the first- and second-order corrections to the ground energy, which are expressed as

$$\varepsilon_g^{(1)} = \langle g | h_1 | g \rangle = zt \sum_{\alpha} \phi_{\alpha}^* \phi_{\alpha}, \quad \alpha = -2, \dots, 2, \quad (20)$$

$$\varepsilon_g^{(2)} = \sum_{n \neq g} \frac{|\langle g | h_1 | m \rangle|^2}{\varepsilon_g^{(0)} - \varepsilon_m^{(0)}} = \sum_{n \neq g} \sum_{\alpha} \frac{z^2 t^2 |\langle g | b_{\alpha} + b_{\alpha}^{\dagger} | m \rangle|^2 \phi_{\alpha}^* \phi_{\alpha}}{\varepsilon_g^{(0)} - \varepsilon_m^{(0)}}, \quad \alpha = -2, \dots, 2. \quad (21)$$

Here  $|g\rangle$  denotes the ground state discussed in the appendix, and  $\{|m\rangle\}$  represent excited states expressed as a cluster of quantum numbers including  $n_0, n_s, F, F_z, \lambda$ . We can calculate all the nonzero matrix elements of  $\langle g|b_\alpha + b_\alpha^\dagger|m\rangle$ . Therefore, second-order perturbation theory gives the form of the modified ground energy as

$$\varepsilon_g = \varepsilon_g^{(0)} + \varepsilon_g^{(1)} + \varepsilon_g^{(2)} = \varepsilon_g^{(0)} + zt \sum_{\alpha} A_{\alpha}(n, \tilde{\mu}, \tilde{c}_0, \tilde{c}_1, \tilde{c}_2, \tilde{p}) \phi_{\alpha}^* \phi_{\alpha}, \quad \alpha = -2, \dots, 2, \quad (22)$$

where  $A_{\alpha}(n, \tilde{\mu}, \tilde{c}_0, \tilde{c}_1, \tilde{c}_2, \tilde{p})$  is related to the first- and second-order corrections of the spin component with magnetic quantum number  $\alpha$  to the zeroth-order ground energy. It depends on system parameters  $n, \tilde{\mu}, \tilde{c}_0, \tilde{c}_1, \tilde{c}_2$  and  $\tilde{p}$ , where  $\tilde{\mu} = \mu/zt, \tilde{c}_0 = c_0/zt, \tilde{c}_1 = c_1/zt, \tilde{c}_2 = c_2/zt, \tilde{p} = p/zt$  are dimensionless. Minimizing the ground energy function Eq. (22), we find that  $\phi_{\alpha} = 0$  when  $A_{\alpha}(n, \tilde{\mu}, \tilde{c}_0, \tilde{c}_1, \tilde{c}_2, \tilde{p}) > 0$  and  $\phi_{\alpha} \neq 0$  when  $A_{\alpha}(n, \tilde{\mu}, \tilde{c}_0, \tilde{c}_1, \tilde{c}_2, \tilde{p}) < 0$ . This means that  $A_{\alpha}(n, \tilde{\mu}, \tilde{c}_0, \tilde{c}_1, \tilde{c}_2, \tilde{p}) = 0$  signifies the boundary between the superfluid and the Mott insulator phases of the spin component with magnetic quantum number  $\alpha$ .

Using the perturbation theory, we can analytically determined the phase diagrams Fig. 1-5 for different cases. The phase diagrams indicate that there exists a phase transition from Mott insulator with integer number bosons to superfluid when the ratio  $c_0/t$  is decreased to a critical value. In the zeroth-order, i.e., neglecting the hopping term, the ground state is Mott state in which the occupation number per site is pinned at integer  $n = 1, 2, \dots$ , corresponding to a commensurate filling of the lattice. Different ground states may contain different spin components. For example, there is only spin component with Zeeman level  $m = 2$  when occupation number per site  $n = 1$ ; spin components with  $m = 0, \pm 1, \pm 2$  for Mott state  $\Pi_i(\hat{A}_0^{(2)}|0\rangle)_i$ , and spin components with  $m = 0, 1, 2$  for  $\Pi_i(\hat{A}_2^{(2)}|0\rangle)_i$ . For the initial Mott ground state including only one spin component, one superfluid component occurs when lowering the ratio  $c_0/t$ , such as the case  $n = 1, 2, 3$  in Fig. 1,  $n = 1, 2$  in Fig. 2, and  $n = 1$  in Fig. 3-5; for all the initial Mott ground states containing multiple spin components, when lowering the ratio  $c_0/t$ , multiple superfluid components appear, and the phase boundaries between superfluid and Mott insulator phase for different spin components are distinct, for instance,  $n = 3$  in Fig. 2,  $n = 2, 3$  in Fig. 3-5. After analyzing the phase diagrams, we find that the position of phase boundary is related to average occupation number of spin component in the initial Mott ground state, i.e., the larger the average occupation number of spin component per site is, the easier the transition from Mott insulator to superfluid phase. We also find that some boundaries between superfluid and Mott insulator phases with multi-spin components, such as  $n = 2$  in Fig. 3,5 and  $n = 3$  in Fig. 3,4, will turn to be identical when the magnetic field vanishes. We can draw the conclusion

that the applied magnetic field results in some phase boundaries splitting.

Furthermore, the phase diagrams Fig. 6(a) and Fig. 6(b) for different intensities of the applied field are drawn. The position of some phase boundaries is related to the intensity of the applied magnetic field. In Fig. 6(a), when the applied magnetic field increases, for the same Mott ground state containing only one spin component with Zeeman level  $m = 2$ , the phase diagrams will shift along the direction with chemical potential decreasing. In Fig. 6(b), for the same Mott ground state containing spin components corresponding to Zeeman levels  $m = 0, \pm 1, \pm 2$ , when the magnetic field increases, the phase boundaries of spin components with Zeeman levels  $m = \pm 1, \pm 2$  move, but the phase boundary of spin component with Zeeman level  $m = 0$  keeps invariant. Moreover, one can see that for positive and negative Zeeman levels, the phase boundaries between SF and MI will move in opposite directions, and for the spin component with positive Zeeman level, the transition from MI to SF becomes easier when the applied magnetic field increases.

## V. REMARKS AND CONCLUSION

For simplicity, in this paper we assume the uniform magnetic field is applied along the  $z$ -direction, and  $p$  is positive. In fact, the analysis of the Mott ground states for  $p > 0$  is enough since the sign of  $p$  does not alter the physics. When  $p < 0$ , the Mott ground states satisfy  $F_z = -F$ , and have the same form as those in the case of  $p > 0$ . We find that the influence of magnetic field on the phase diagrams is manifold, and the boundaries between SF and MI are essentially dependent on the magnetic properties of the ground states. This work only discuss the phase diagrams corresponding to different magnetic fields with the same Mott ground state, i.e., the continuous change of the phase boundaries. The case that Mott ground states change when the magnetic field increases, i.e., the sudden jump of the phase boundaries, is beyond the scope of the present paper and is not shown. For instance, when  $c_1 > 0$ ,  $c_2 > 0$ , if  $p$  increases from 0 to the value large enough to satisfy  $p/(2n + 1) > c_1$ , the magnetization  $F$  can jump from the minimum to the maximum one. They are the subject of future study. In addition, it is worth to note that phase diagrams of the zero magnetic field cannot be derived by taking  $p = 0$  simply, since our derivation is based on the degeneracy lifting.

In conclusion, we have investigated the quantum phase transition from Mott insulator to superfluid phase of spin-2 cold bosons with repulsive interaction in optical lattices under the influence of a uniform magnetic field at zero temperature. The phase diagrams show that

the system undergoes a phase transition from Mott insulator with integer number bosons at each site to superfluid phase when the ratio  $c_0/t$  is decreased to a critical value. Different Mott ground states may contain different spin components. The position of phase boundary is related to average occupation number of spin component in the initial Mott ground state. For the initial Mott ground state including only one spin component, one superfluid component appears when lowering the ratio  $c_0/t$ . For some Mott ground states with multiple spin components, the applied magnetic field leads to the splitting of the phase boundaries, so that the phase boundaries between superfluid and Mott-insulator phase for different spin components are distinct in all ground states. In particular, we draw the phase diagrams corresponding to different intensities magnetic field for the initial Mott ground state containing one-spin and multi-spin components. They qualitatively show the way of the phase boundaries' moving with the intensity of the applied magnetic field. It is found that the phase boundaries can be moved by only changing the intensity of the applied magnetic field. For the spin component with positive Zeeman level, the larger intensity of the magnetic field is, the easier the transition from MI to SF happens. These theoretical results are expected to be practically helpful to the experimental study of the field-tuned SF-MI transition of bose atoms with hyperfine spin in an optical lattice.

### Acknowledgments

This work is in part supported by NSF of China Grant No.A0124015.

### APPENDIX: LIST OF THE MOTT GROUND STATES

1.  $c_1 < 0, c_2 > 0$ . Because  $(2p - c_1)/(2c_1) \leq 0$ , the third term and the fourth term in Eq. (19) have the minimal values at the same time when  $F = 2n$  and  $n_s = 0$ . Hence, the ground state is  $|n, 0, 2n, 2n; \lambda\rangle$ .
2.  $c_1 < 0, c_2 < 0$ . The relation  $(2p - c_1)/(2c_1) \leq 0$  stands, and the competition between contributions of total spin and the singlet “pair” happens in the premise of  $\frac{F}{2} + 2n_s = n$ . If we skip over the fact for the moment that the singlet “pair” number  $n_s$  is an integer, then the condition to minimize the energy function is given by

$$n_s = \frac{10c_1(4n + 1) - c_2(2n + 3) - 20c_1p}{80c_1 - 4c_2}. \quad (\text{A.1})$$

Because the singlet “pair” number must be an integer, we write  $n_s$  in terms of the closest integer number  $n_s^0$  and the decimal part, i.e.  $n_s = n_s^0 + \alpha$ , where the number  $\alpha$  satisfies  $-1/2 < \alpha < 1/2$ , which can be rewritten as,

$$n_s^0 - \frac{1}{2} < \frac{10c_1(4n+1) - c_2(2n+3) - 20c_1p}{80c_1 - 4c_2} < n_s^0 + \frac{1}{2}. \quad (\text{A.2})$$

- (a) Because the singlet “pair” number is not negative,  $n_s$  must be zero for  $n_s^0 \leq 0$ . Hence, the ground state is  $|n, 0, 2n, 2n; \lambda\rangle$ .
- (b) For  $0 < n_s^0 < \frac{n}{2}$ , the eigenenergy is lower when the singlet “pair” number is  $n_s^0$  than any other integer. So the ground state is  $|n - 2n_s^0, n_s^0, 2n - 4n_s^0, 2n - 4n_s^0; \lambda\rangle$ .
- (c) For  $n_s^0 \geq \frac{n}{2}$ , the singlet “pair” number takes the highest value as it can. (i) When  $n$  is even, the ground state is  $|0, n/2, 0, 0; \lambda\rangle$ ; (ii) when  $n$  is odd, the ground state is  $|1, (n-1)/2, 2, 2; \lambda\rangle$ .

3.  $c_1 > 0, c_2 > 0$ . For convenience, we introduce a new parameter

$$F_1 = \frac{2p - c_1}{2c_1} = F_0 + \alpha, \quad (\text{A.3})$$

where  $F_0$  is the integer number which is the closest integer to  $F_1$ . In Eq. (19), when  $n_s = 0$  the fourth term has the minimal value, and if total spin  $F$  takes the appropriate integer the third term possesses the minimal one.

- (a) When  $F_0 \leq 0$ , i.e.,  $c_1 > p$ , the energy eigenvalue has its minimum if  $F = 0$  and  $n_s = 0$ . However, we must notice some special cases because there have some forbidden values [17, 18], that is,  $F = 1, 2, 5, 2n_0 - 1$  are not allowed when  $n_0 = 3k(k \in \mathbb{Z})$ , and  $F = 0, 1, 3, 2n_0 - 1$  are forbidden when  $n_0 = 3k \pm 1(k \in \mathbb{Z})$ .
  - i. For  $n = 3k(k \in \mathbb{Z})$ ,  $|n, 0, 0, 0; \lambda\rangle$  with  $n_s = 0$  and  $F = 0$  is the ground state.
  - ii. For  $n = 3k - 1(k \in \mathbb{Z})$ , the state with  $n_s = 0$  and  $F = 0$  is not allowed simultaneously. If  $n_s = 0$ , the lowest allowed value of total spin  $F$  is 2. On the other hand,  $F = 0$  is not forbidden when  $n_0$  is  $3k(k \in \mathbb{Z})$ .  $n_s = 1$  is the lowest value satisfying the condition due to  $n = 2n_s + n_0$ . So the state with  $n_s = 1$  and  $F = 0$  is a possible ground state. Comparing both eigenenergies for the two cases  $F = 0, n_s = 1$  and  $F = 2, n_s = 0$ , we get the ground state, (i)  $|n - 2, 1, 0, 0; \lambda\rangle$  for  $c_2 < (15c_1 - 10p)/(2n + 1)$  and (ii)  $|n, 0, 2, 2; \lambda\rangle$  for  $c_2 > (15c_1 - 10p)/(2n + 1)$ .

iii. For  $n = 3k+1$  ( $k \in \mathbb{Z}$ ), the competition exists between contributions of total spin and the singlet “pair” to eigenenergy. But if  $F = 0$ ,  $n_s$  is at least 2. Therefore, the ground state is (i)  $|n-4, 2, 0, 0; \lambda\rangle$  for  $c_2 < (15c_1 - 10p)/2(2n-1)$ ; (ii)  $|n, 0, 2, 2; \lambda\rangle$  for  $c_2 > (15c_1 - 10p)/2(2n-1)$ .

(b) When  $F_0 \geq 2n$ , i.e.,  $c_1 < p/(2n+1)$ , the ground state is  $|n, 0, 2n, 2n; \lambda\rangle$  with  $F = 2n$  and  $n_s = 0$ .

(c) When  $0 < F_0 < 2n$ , i.e.,  $p/(2n+1) < c_1 < p$ , the eigenenergy is thus lower when  $F$  is closer to  $F_1$  and when  $n_s$  is smaller. Except for the case of  $F_0$  taking the forbidden values of  $F$ , the ground state is  $|n, 0, F_0, F_0; \lambda\rangle$ . When  $F_0$  equals to the forbidden values of  $F$ ,  $F$  may take the allowed integer next-nearest to  $F_1$ , i.e.,  $F_0 \pm 1$  or  $F_0 \pm 2$ , or at the cost of increasing  $n_s$  to 1 or 2, since any of the three values 0, 1, 2 of  $n_0 \bmod 3$  is realized by setting  $n_s$  as 0, 1, or 2 owing to the relation  $n = 2n_s + n_0$ . Whether or not the states  $|n, 0, F_0 \pm 1, F_0 \pm 1; \lambda\rangle$ ,  $|n, 0, F_0 \pm 2, F_0 \pm 2; \lambda\rangle$ ,  $|n-2, 1, F_0, F_0; \lambda\rangle$ , and  $|n-4, 2, F_0, F_0; \lambda\rangle$  can be the lowest-energy state depends on the ratio  $c_2/c_1$ .

4.  $c_1 > 0$ ,  $c_2 < 0$ . The eigenenergy is the lowest if  $F = F_0$  and  $n_s$  at its highest value. However, these two choices are not always satisfied simultaneously.

(a)  $F_0 \leq 0$ , i.e.,  $c_1 > p$ .

- i. When  $n$  is even,  $|0, n/2, 0, 0; \lambda\rangle$  is the ground state.
- ii. When  $n$  is odd,  $n_s$  has the highest value  $(n-1)/2$ . But  $F$  is not zero when  $n_s = (n-1)/2$ . Alternatively, there is another case that  $F = 0$  and  $n_s = (n-3)/2$ . Hence, the ground state is (i)  $|1, (n-1)/2, 2, 2; \lambda\rangle$  for  $c_1 < (7|c_2| + 10p)/15$ ; (ii)  $|3, (n-3)/2, 0, 0; \lambda\rangle$  for  $c_1 > (7|c_2| + 10p)/15$ .

(b)  $F_0 > 0$ , i.e.,  $c_1 < p$ . Note that  $n_s^0$  is shown in Eq. (A.2), similar to the analysis of case 2., it is divided into three cases.

- i. For  $n_s^0 \leq 0$ , the ground state is  $|n, 0, 2n, 2n; \lambda\rangle$ .
- ii. For  $0 < n_s^0 < \frac{n}{2}$ , the ground state is  $|n-2n_s^0, n_s^0, 2n-4n_s^0, 2n-4n_s^0; \lambda\rangle$ .
- iii. For  $n_s^0 \geq \frac{n}{2}$ , (i) when  $n$  is even,  $|0, n/2, 0, 0; \lambda\rangle$  is the ground state; (ii) when  $n$  is odd,  $|1, (n-1)/2, 2, 2; \lambda\rangle$  does.

---

- [1] B. P. Anderson, M. A. Kasevich, *Science* **282** (1998) 1686.
- [2] C. Orzel *et al.*, *Science* **291** (2001) 2386.
- [3] M. Greiner *et al.*, *Nature* **415** 39 (2002).
- [4] M. Greiner *et al.*, *Nature* **419** 51 (2002).
- [5] G. Grynberg *et al.*, *Phys. Rev. Lett.* **70** 2249 (1993).
- [6] P. S. Jessen and I. H. Deutsch, *Adv. in At, Mol. and Opt. Phys.* **37** 95 (1996).
- [7] D. Jaksch, C. Bruder, J. I. Cirac, C. W. Gardiner, and P. Zoller, *Phys. Rev. Lett.* **81** 3108 (1998).
- [8] M. P. A. Fisher, P. B. Weichman, G. Grinstein and D. S. Fisher, *Phys. Rev. B* **40** 546 (1989).
- [9] D. van Oosten, P. van der Straten and H. T. C. Stoof, *Phys. Rev. A* **63** 053601 (2001).
- [10] G. H. Chen and Y. S. Wu *Phys. Rev. A* **67** 013606 (2003).
- [11] D. M. Stamper-Kurn *et al.*, *Phys. Rev. Lett.* **80** 2027 (1998).
- [12] J. Stenger *et al.*, *Nature (London)* **396** 345 (1999).
- [13] M. D. Barrett, J. A. Sauer, and M. S. Chapman, *Phys. Rev. Lett.* **87** 010404 (2001).
- [14] T. L. Ho, *Phys. Rev. Lett.* **81** 742 (1998).
- [15] T. Ohmi and K. Machida, *J. Phys. Soc. Jpn.* **67** 1822 (1998).
- [16] C. V. Ciobanu, S. K. Yip and T. L. Ho, *Phys. Rev. A* **61** 033607 (2000).
- [17] M. Koashi and M. Ueda, *Phys. Rev. Lett.* **84** 1066 (2000).
- [18] M. Ueda and M. Koashi, *Phys. Rev. A* **65** 063602 (2002).
- [19] E. Demler and F. Zhou, *Phys. Rev. Lett.* **88** 163001 (2002).
- [20] S. Tsuchiya, S. Kurihara, and T. Kimura, e-print cond-mat/0209676.
- [21] J. M. Hou and M. L. Ge, *Phys. Rev. A* **67** 063607 (2003).
- [22] E. N. Bulgakov and A. F. Sadreev, *Phys. Rev. Lett.* **90** 200401 (2003).
- [23] R. A. Duine and H. T. C. Stoof, *Phys. Rev. A* **68** 013602 (2003). 063610 (2002).
- [24] P. Zhang *et al.*, *Phys. Rev. A* **66** 043606 (2002).
- [25] G. M. Genkin, *Phys. Rev. A* **63** 025602 (2001).
- [26] A. Yazdani and A. Kapitulnik, *Phys. Rev. Lett.* **74** 3037 (1995).
- [27] H. S. J. van der Zant *et al.*, *Phys. Rev. Lett.* **69** 2971 (1992).
- [28] A. F. Hebard and M. A. Paalanen, *Phys. Rev. Lett.* **65** 927 (1990).
- [29] B. Pannetier *et al.*, *Phys. Rev. Lett.* **53** 1845 (1984).
- [30] A. A. Svicainsky and S. T. Chui, *Phys. Rev. A* **68** 043612 (2003).

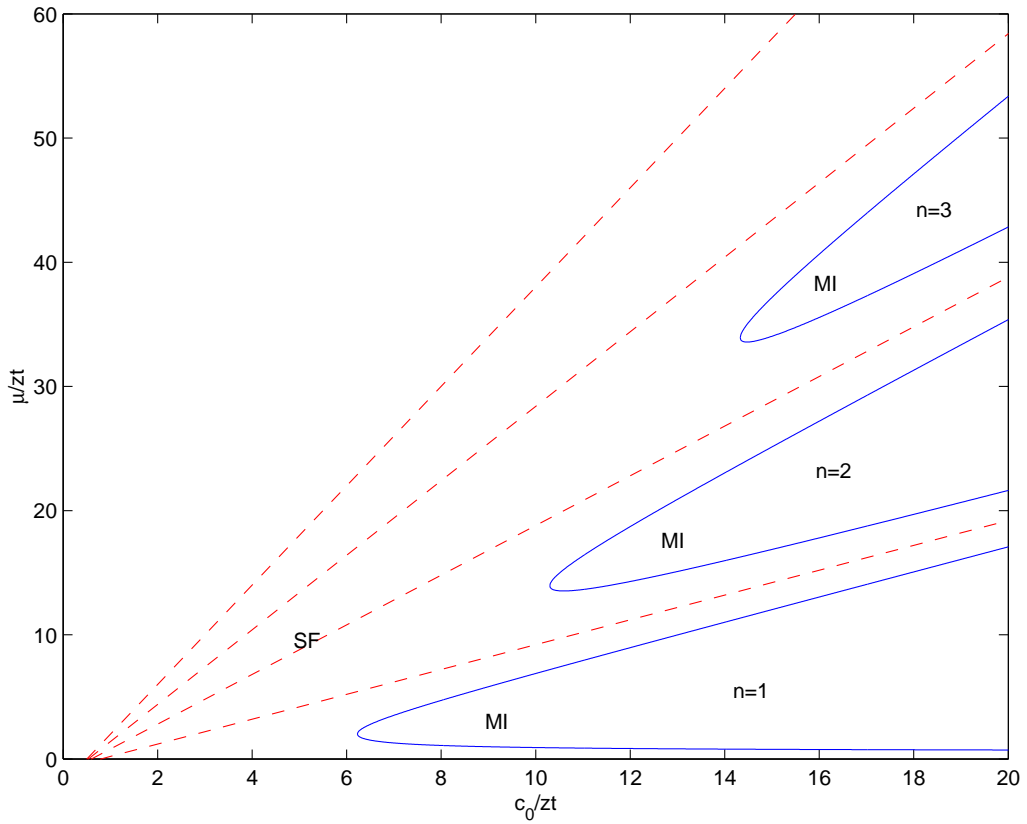


FIG. 1: The phase diagram of Bose-Hubbard Hamiltonian obtained from second-order perturbation theory with solid lines for  $c_1 = -0.1zt$ ,  $c_2 = 0.1zt$  and  $p = 0.2zt$ . The dashed lines indicate the zeroth-order phase diagram.

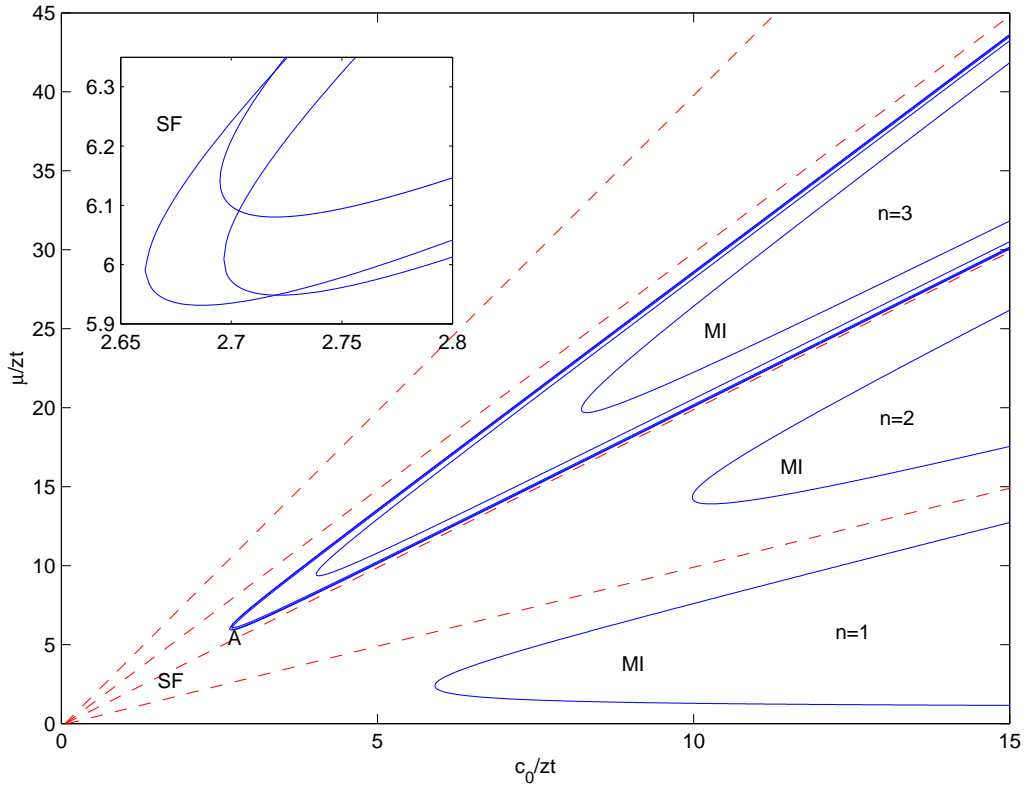


FIG. 2: The same as in Fig.1, but for  $c_1 = -0.02zt$ ,  $c_2 = -0.25zt$  and  $p = 0.01zt$  with solid lines. For  $n = 3$ , the interior line is the phase boundary of spin component with Zeeman level  $m = 2$ ; the middle line the phase boundary of spin component with Zeeman level  $m = -2$ , and the external triple lines, which are too close to be distinguished, the phase boundaries of spin components with Zeeman levels  $m = 0, \pm 1$ . The inset shows an expansion of the region labelled by A.

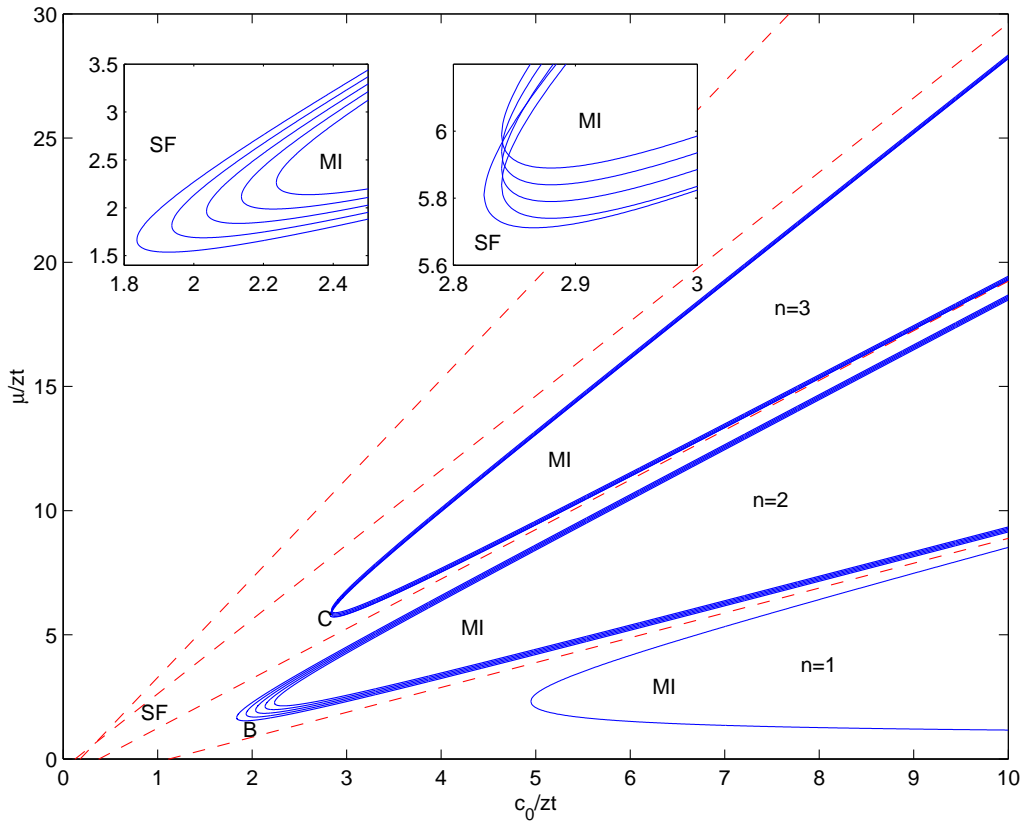


FIG. 3: The same as in Fig.1, but for  $c_1 = 0.22zt$ ,  $c_2 = 0.1zt$  and  $p = 0.05zt$  with solid lines. When  $n = 2$ , the region labelled by B is enlarged in the left inset; the five lines represent the phase boundaries of spin components with Zeeman levels  $m = -2, -1, 0, 1, 2$  respectively (from interior to external). For  $n = 3$ , the five lines are too close to be distinguished, so the region labelled by C is enlarged in the right inset, in which the five lines the phase boundaries of spin components with Zeeman levels  $m = 0, \pm 1, \pm 2$ .

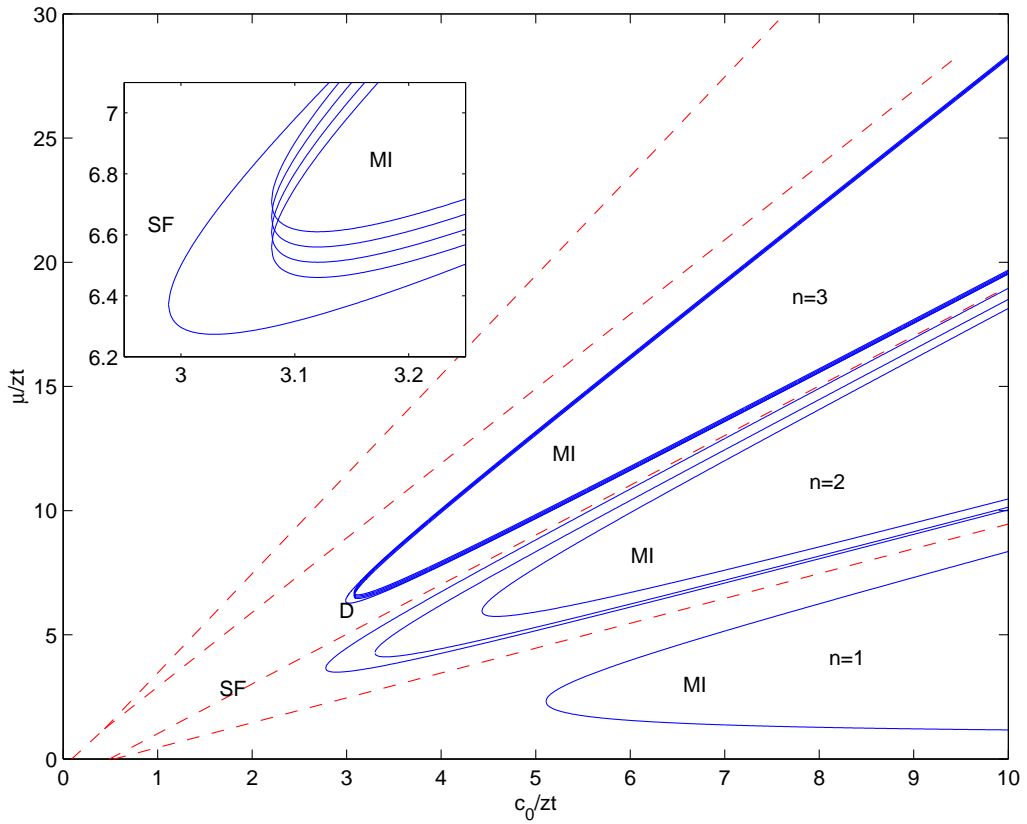


FIG. 4: The same as in Fig.1, but for  $c_1 = 0.18zt$ ,  $c_2 = 1.0zt$  and  $p = 0.05zt$  with solid lines. For  $n = 2$ , the three lines represent the phase boundaries of spin components with Zeeman level  $m = 1, 0, 2$  respectively (from interior to external). When  $n = 3$ , the five lines are too close to be distinguished, so the region labelled by D is enlarged in the inset, in which the external line is the phase boundary of spin component with Zeeman level  $m = 2$ , and the other four lines the phase boundaries of spin components with Zeeman levels  $m = 0, \pm 1, -2$ .

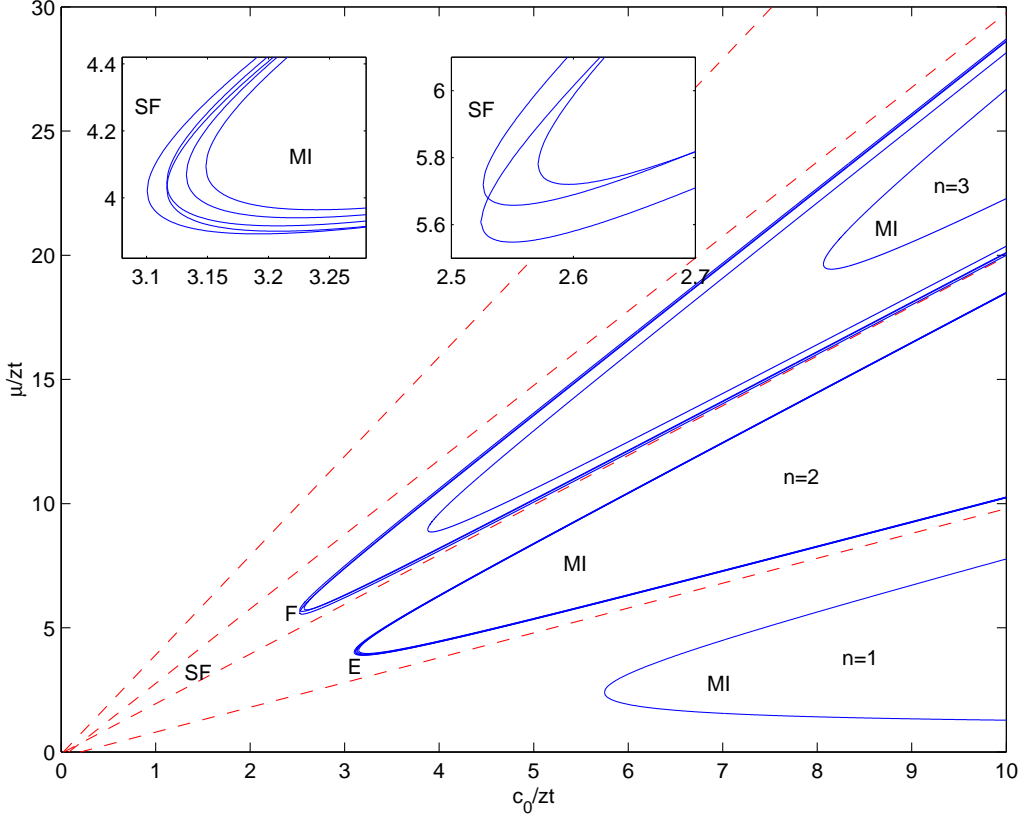


FIG. 5: The same as in Fig.1, but for  $c_1 = 0.02zt$ ,  $c_2 = -0.1zt$  and  $p = 0.008zt$  with solid lines. When  $n = 2$ , the five lines are too close to be distinguished, so the region labelled by E is extended in the left inset, in which the interior line is the phase boundary of spin component with Zeeman level  $m = -1$ ; the external line the phase boundary of spin component with Zeeman level  $m = 1$ ; the three middle lines the phase boundaries of spin components with Zeeman levels  $m = 0, \pm 2$ . For  $n = 3$ , the exterior line is the phase boundary of spin component with Zeeman level  $m = 2$ ; the middle line the phase boundary of spin component with Zeeman level  $m = -2$ , and the external triple lines, which are too close to be distinguished, the phase boundaries of spin components with Zeeman levels  $m = 0, \pm 1$ . The right inset shows an expansion of the region labelled by F.

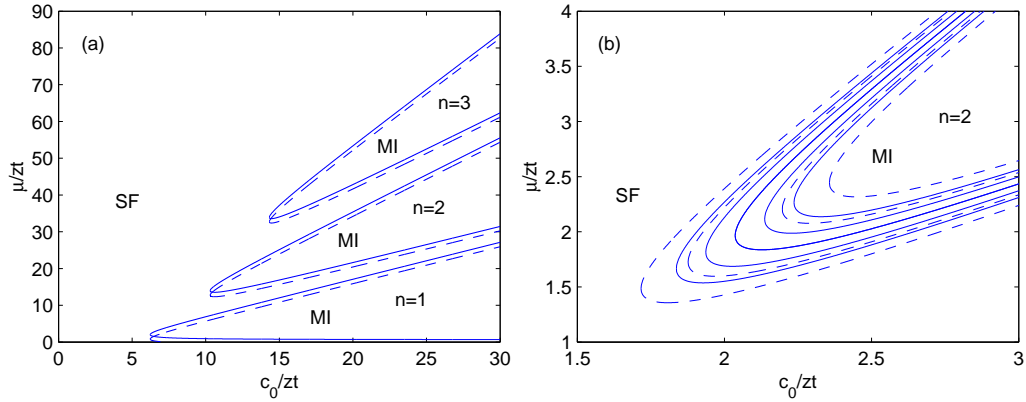


FIG. 6: The phase diagrams of Bose-Hubbard Hamiltonian obtained from second-order perturbation theory for different  $p$ . In (a),  $c_1 = -0.1zt$ ,  $c_2 = 0.1zt$ , with  $p = 0.2zt$  (solid lines) and  $p = 0.8zt$  (dashed lines) respectively. In (b), when  $n = 2$ ,  $c_1 = 0.22zt$ ,  $c_2 = 0.1zt$ , with  $p = 0.05zt$  (solid lines) and  $p = 0.08zt$  (dashed lines) respectively; the middle solid line expresses the phase boundary of spin component with Zeeman level  $m = 0$ , and keeps invariant when  $p = 0.08zt$ ; the five solid lines represent the phase boundaries of spin components with Zeeman levels  $m = -2, -1, 0, 1, 2$  respectively (from interior to external); the four dashed lines represent the phase boundaries of spin components with Zeeman levels  $m = -2, -1, 1, 2$  respectively (from interior to external).